Magnetic properties and microstructure of FePt (BN/AlN, Ag, C) film

Jai-Lin Tsai*, Cheng-Yu Tsai, Mau-Tin Lin, Yi-Yuan Huang, Hsin-Hau Huang
Department of Materials Science and Engineering, National Chung Hsing University, Taichung 40227, Taiwan, tsaijl@dragon.nchu.edu.tw

The FePt (BN/AlN, Ag, C) and FePt (BN, Ag, C) films illustrate close ordering degrees (0.84), which means the hard L1$_0$ FePt phase is almost equal in both films. The FePt (BN/AlN, Ag, C) film has a higher c-axis alignment, evidenced in the lower rocking width in (001)/(002) (=3.94°/2.5°) diffraction peaks. The more c-axis anisotropic crystal grains also respond to the higher nucleation field, magneto-crystalline anisotropy, and lower hard-/easy-axis remanence ratio than the reference sample. The FePt (BN, Ag, C) film presents large perpendicular magnetic anisotropy and out-of-plane coercivity (31.7 kOe). Still, the disordered fcc FePt contributed to the in-plane magnetization and wider hard-axis hysteresis loop. However, the out-of-plane coercivity is much smaller in the FePt (BN/AlN, Ag, C) film (16.7 kOe) due to the formation of soft magnetic FeB grains and the hard- and soft-magnetic phases are exchange-coupled, which enhances the magnetic remanence and saturation magnetization. From microstructure image mapping, AlN segregated at the grains boundaries, but part of Al was presented in the FePt lattice and was supposed to initiate the formation of FeB due to high atomic diffusivity at high deposition temperature.

Index Terms—**perpendicular magnetic anisotropy, out-of-plane coercivity, exchange-coupled grains.**

I. Introduction

In conventional CoCrPt-oxides based media, the non-magnetic exchange control layer was used to adjust the interlayer and lateral grain interaction in the magnetic layer which has gradient perpendicular magnetic anisotropy (PMA) to increase the signal-to-noise ratio. The ordered FePt-based media with gradient PMA is also required for heat-assisted magnetic recording (HAMR) media to control the read/write physical-related parameters. The compositional variation in the L1$_0$-FePt layer can change the ordering degree and magneto-crystalline anisotropy (K_u) intrinsically, and the grains-isolated materials (segregants) can also influence the magnetic properties extrinsically [1].

From microstructure and surface roughness, segregants are required to form a granular structure in which L1$_0$ FePt grains are in the matrix and amorphous BN, and carbon are in the grain boundaries. Here, BN is mechanically hard to grow the FePt columnar grains. However, the lower deposition rate causes inclined and interrupted columnar grains with different grain aspect ratios. The AlN nitride has much higher thermal conductivity and lower electric resistivity, which were doped to replace half of the BN in FePt (BN, Ag, C) film, obtaining different magnetic properties and microstructure. For segregants in HAMR media, the higher thermal conductivity is not beneficial for the thermal insulating boundary during thermal writing, and lower electric resistivity is better for the sputtering process to avoid particles. This study will extensively discuss the magnetic properties and microstructure of the FePt (BN/AlN, Ag, C) film and reference sample.

II. Experimental

The FePt (BN, Ag, C) and FePt (BN/AlN, Ag, C) thin films were prepared on the MgO (100) single-crystal substrate by direct current (DC) magnetron sputtering. The thin film deposition system was designed to have a pre-chamber which was used to transfer the substrate from the atmosphere end by load-lock feedthrough to keep the high vacuum pressure in the main main-chambers which installed four sputtering cathodes (AJA, A320, MA, USA), including gas line and lamp heated substrate holder (OSRAM, 1000W). The composite targets FePt(BN, Ag, C) (reference composition) and FePt(BN/AlN, Ag, C) with two-inch-diameter were manufactured and used. In this study, half BN was replaced by AlN and compared the AlN replacement effects on magnetic properties and microstructure. Further, the MgO (100) single crystal was chosed to provide the stable baseline for the epitaxial growth of (001) textured FePt film. The MgO (100) substrate (HF-Kejing, 10x10x0.5mm) was heated at 470 °C (real sample surface temperature after calibration) for dry cleaning and then the magnetic layers with thickness of 15 nm were sputtered under an Ar working pressure of 10 mTorr at the same temperature by the composite targets. The deposition rate of FePt (BN, Ag, C) (15nm) and FePt (BN/AlN, Ag, C) (15nm) was 0.069 nm/s and 0.005 nm/s, respectively.

The crystal structure was measured using standard X-ray diffraction (XRD) (BRUKER, D8 Discover). The magnetization curves with in-plane and out-of-plane measured hysteresis loops were performed with a superconducting quantum interference device (SQUID) magnetometer (MPMS-XL). The sample microstructure was observed using transmission electron microscopy (TEM, JEOL JEM-2010).

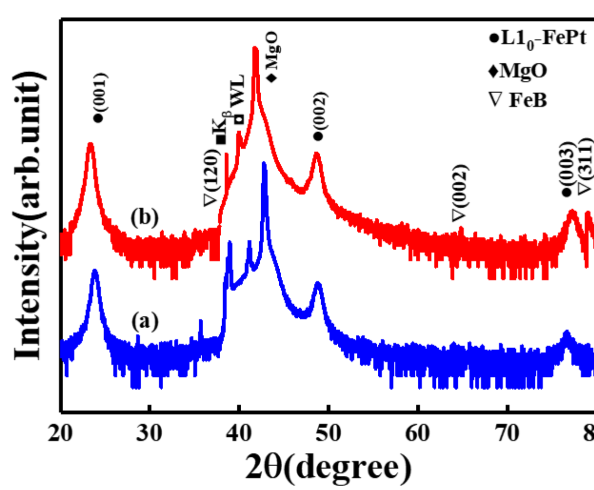

Fig. 1. XRD pattern of (a) FePt (BN, Ag, C) and (b) FePt (BN/AlN, Ag, C) films

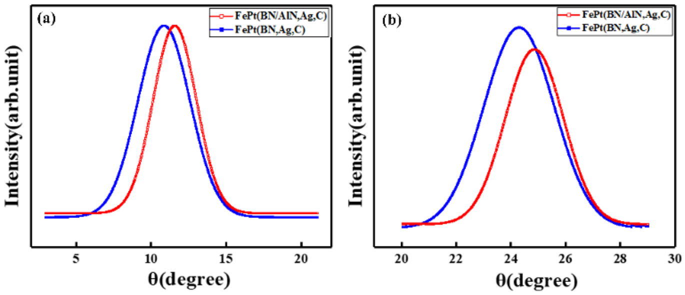

Fig. 2 Rocking curves of $L1_0$ FePt (a) (001), and (b) (002) diffraction peaks for FePt (BN, Ag, C) and FePt (BN/AlN, Ag, C) films

III. Results and Discussion

Figure 1 shows the x-ray diffraction (XRD) patterns of the FePt (BN, Ag, C) and FePt (BN/AlN, Ag, C) films presented by the log scale. The ordered FePt superlattice peaks presented by (001) and (003) and fundamental diffraction peaks presented by (002) were all indexed, and the MgO (002) peak from single crystal substrate and Cu K_β radiation (~38°) and tungsten (W) filament signal (~41°) from x-ray source tube were all observed apparently. For the soft magnetic phase, the disordered face-centered cubic (fcc) FePt (200) peak was almost neglected, and the FeB (120), (002) and (311) peaks were indexed in FePt(BN/AlN, Ag, C) film in Fig. 1(b). Figure 2 illustrates the $L1_0$-FePt (001)/(002) rocking curves, and the rocking width (full width of half maximum, FWHM, $\Delta\theta_{50}$) are 4.09°/3.03° and 3.94°/ 2.50° for reference film and FePt (BN/AlN, Ag, C) film, respectively, and the crystallinity and c-axis alignment of later is better. Due to the strong $L1_0$ FePt [001] texture, both films show high perpendicular magnetic anisotropy, with high perpendicular magnetization along the c-axis (out-of-plane) and low remanence in the film plane in Fig. 3. The FePt (BN/AlN, Ag, C) film shows a higher nucleation field (-5.67 > -2.53 kOe), magnetocrystalline anisotropy ($1.84\text{x}10^7 > 1.74\text{x}10^7$ erg/cm^3), lower in-plane H_c (1.3<4.5 kOe) and hard-/easy-axis remanence ratio (0.073<0.121) than the reference sample. However, the FePt (BN/AlN, Ag, C) shows much lower out-of-plane H_c than the reference sample (16.7<31.7 kOe) and higher saturation magnetization (M_s, 544>502 emu/cm^3) and magnetic remanence (M_r, 479>462 emu/cm^3) due to the exchange-coupled hard-/soft-magnetic $L1_0$ FePt/FeB grains.

For the plane-view TEM images observed in bright field mode illustrated in Fig. 4, the reference and FePt(BN/AlN, Ag, C) films presented a typical granular microstructure where the core FePt grains were surrounded by the grain boundary materials (C, BN, AlN). These magnetic grain sizes have gauss

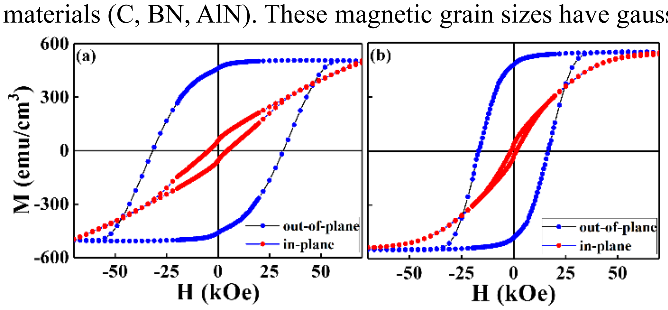

Fig. 3 Magnetic hysteresis loops measured out-of-plane and in-plane for (a) FePt (BN, Ag, C) and FePt (BN/AlN, Ag, C) films

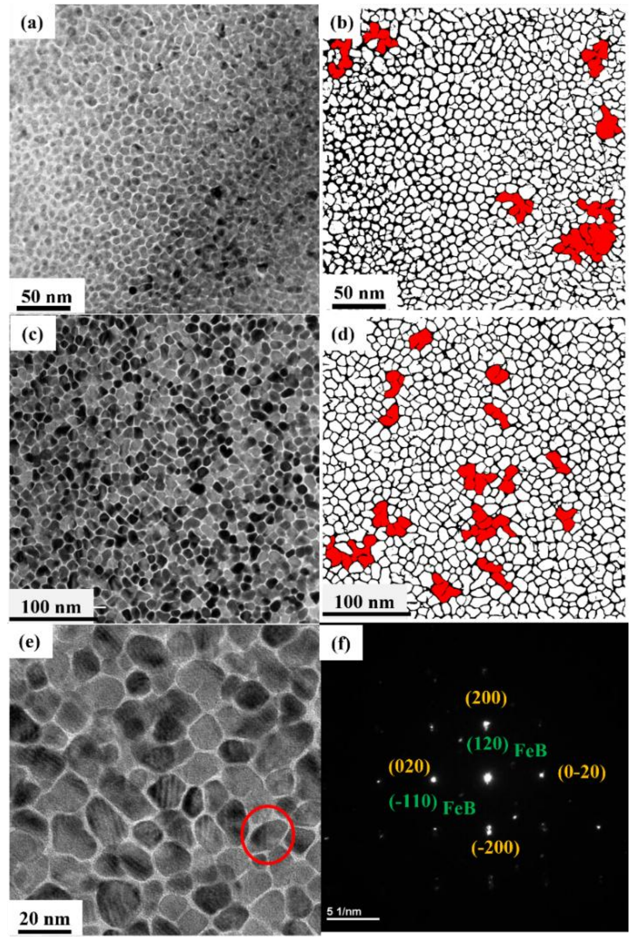

Fig. 4 The plane-view bright-field TEM images of (a) FePt(BN, Ag, C) film, (b) image segmentation of (a), (c) FePt(BN/AlN, Ag, C) film, (d) image segmentation of (c), (e) image with L10FePt-FeB grains (circle area), (f) nano-beam diffraction of circle area

distribution with average grains size <D> of 8.15 nm, and 10.8 nm, respectively, estimated by programming counting 823, and 867 grains. The distributed grains size was calculated by the standard deviation (σ) divided by the average grains size <D> with the values of 37.5 % and 33.7%. The averages of large numbers of grains were estimated by using the segmentation of TEM in-plane grains images, which was produced by the neuro network-like deep learning trained model (U-net). The highlighted grains belong to the interconnected L10 FePt grains in the reference sample and are supposed to be the FeB/L10 FePt exchange coupled grains in the FePt(BN/AlN, Ag, C) film, which has larger red areas.

To prove the FeB/$L1_0$ FePt) exchange-coupled grains, the nanobeam diffraction was performed on different grains in Fig. 5, and despite the $L1_0$ FePt {200} plane, the FeB (120) and (110) planes were also indexed in the nanobeam diffraction pattern in (b). Further, the negative formation energy (-0.38 eV/atom) of FeB also explained the formation tendency from thermodynamics.

References

[1] Jai-Lin Tsai*, Jhih-Hong Lin, Tsung-Yi Chen , Yu-Chun Lin , Li-Xiang Liu, Ming-Wei Hsieh, Jyun-you Chen, "Segregation effects of doped VN and ZrN on magnetic and microstructural characteristics of FePt-based films", Thin. Solid. Films 798, 140376-1-11 (2024).